Composite Materials
2020; 4(1): 1-7
http://www.sciencepublishinggroup.com/j/cm
doi: 10.11648/j.cm.20200401.11

Walnut Inspired Silicon Carbon Composites for Stable Lithium Ions Battery Anodes

Xuli Ding[1, *], Daowei Liang[1], Yi Liu[2]

[1]School of Science, Jiangsu University of Science and Technology, Zhenjiang, The People's Republic of China

[2]Shanghai Synchrotron Radiation Facility, Chinese Academy of Science, Shanghai, The People's Republic of China

Email address:
xuliding@just.edu.cn (Xuli Ding)

[*]Corresponding author

To cite this article:
Xuli Ding, Daowei Liang, Yi Liu. Walnut Inspired Silicon Carbon Composites for Stable Lithium Ions Battery Anodes. *Composite Materials.* Vol. 4, No. 1, 2020, pp. 1-7. doi: 10.11648/j.cm.20200401.11

Received: November 29, 2019; **Accepted**: December 21, 2019; **Published**: January 6, 2020

Abstract: The distinct quality of silicon (Si) makes it a natural choice for employment as a competitive anode material in rechargeable high specific energy lithium-ion batteries (LIBs) for practical applications. However, the Si-based LIBs are still hindered for practical applications due to the weak electrical conductivity and unstable solid electrolyte interfaces (SEI). New structures with enhanced conduction are highly desired to push the advance of Si-based LIBs. Herein, the Si nanoparticles coated by few-layer graphene (fGra) has been wrapped into honeycomb porous carbon (Pc) framework with good Si-C contact and reliable void via a simple chemical vapor deposition accompanying with freeze drying strategy. The walnut-type structure noted as Si@Gra@Pc is obtained, in which the porous architecture not only shorten the transfer distance of the lithium ions but also provide good electrical conductivity for the charge carriers. Moreover, the porous structure permit the free expansion of Si during charging/discharging cycling and preserve the integrity of the electrode owing to the brawny mechanical strength of Gra and Pc framework. Importantly, it is found that the Si@Gra@Pc composites show good rate capability reached to $5Ag^{-1}$ with specific capacity of 450 mAh g^{-1} and good cycling stability with no distinct capacity decay even after 1000 cycles, which are obvious improving compared with that of the bare Si anodes. Combined with the simple and feasible fabrication method and improved electrochemical performance for the Si anodes in LIBs. The present walnut-type Si@Gra@Pc composite is considered as the promising and meaningful Si-based anode materials and candidates in the development of next-generation high specific energy LIBs.

Keywords: Silicon, Lithium-ion Battery, Anode, Graphene, CVD

1. Introduction

It is universal call for the advanced Li-ion batteries (LIBs) with higher energy/power density, faster electrons/ions kinetics and lower cost for the fast-developing electronic devices [1-3]. The anode and cathode materials play pivotal roles in the further improving the battery energy storage performance [4-9]. Various efforts have been devoted to explore the better battery materials, among them, tetrahedral silicon (Si) has motivated more interest as promising candidate for the next-generation high specific energy LIBs to meet the goal of the vehicle electrification, due to its high capacity (4200 mAh g^{-1}), low cost and environmental compatibility [10-14]. However, Si-based anodes have been hindered suffering the fast capacity fade under charging/discharging at high rates due to the slow diffusion of Li^+ ions and electrons, caused by the poor electrical conductivity ($1.56\times10^{-3}Sm^{-1}$) of Si, large volume change (~400%) for lithiation and instable solid-electrolyte interphase (SEI) with the repeated cycles. Enormous strategies have been adopted to tackle the above-mentioned challenges [15-20]. Among those, the nano Si with original Si-C composite structures can present the promising opportunity due to the more faster ions kinetics and lower cost [21-25]. But the main challenges associated with the Si-based anodes are still how to better electrically connect among Si nanoparticles, how to maintain more stable structure for the repetitive cycling, and how to accommodate the large volume expansion during lithiation [26-29]. To exceed these issues and improve the entire energy storage performance of the Si-based anodes, one effective strategy is to synthesis composite nanostructures by nano-engineering, which is key to enhance the cycle-life and the rate capability. To develop desirable nano Si-C anodes, the

following strategies should be considered: (1) the high electro-conductive and elastic fundus provided to improve the conductivity and buffer the volume changes, (2) the nano-Si surface protection designed to facilitate the formation of thin and beefy SEI to reduce the irreversible capacity loss, (3) the ideal Si-C composite with good contact interfaces and accommodative porous spaces. Herein, we propose a neoteric Si@Gra inlayed in the honeycomb carbon, consisting of Si particles wraped with few-layer Gra and then wrapped by the honeycomb porous carbon (Pc) skeletons (abbreviated as Si@Gra@Pc) forming walnut-like nanostructures, in which the Si@Gra particles are the core of the walnut and the Pc is the shell of the walnut. This structure can not only help the in-depth understanding of unusual features of the transport and storage behaviors of ions at atomic scale, but also may orient super advanced energy storage devices, in which the Si@Gra has soft Gra protective interface with a stable SEI layer for the repetitive cycles. Particularly, a). the few-layer Gra protected Si from direct exposing to electrolyte; b). the meso/macro pore carbon network enpowers the rapid ions transport and buffers the stress during the repeated Li^+ insertion/extraction to maintain the structural integrity; c). the highly conductive ability of the Gra and Pc facilitates the fast electron transfer between the active particles and the current collector. The fabricated Si@Gra@Pc anode was tested to achieve good rate capacity and cycling stability (90% retention after 1000 cycles at $1Ag^{-1}$).

2. Experimental Section

The preparation process of Si@Gra@Pc is shown in Figure 1. Firstly, few-layer graphene was grown on the surface of Si nanoparticles (50-100 nm in diameter, Shanghai Haotian Nano Company) by atmospheric pressure CVD to obtain Si@Gra samples, and then the Si@Gra nanoparticles were dispersed in an aqueous solution of chitosan in the deionized water and stired the mixture for 10h. The methane was used for the few-layer graphene growth in the CVD process, the growth temperature was 1000°C, and the growth time was 30 min. Secondly, the mixture was freeze-dried under vacuum for 24h to obtain the porous structure, during which the Si@Gra@Pc composites were obtained by mixing the alcohol and chitosan composites suspension with volume ratio of 1:1 deionized water and stirring for 10h at 50°C to evaporate the alcohol, followed by freeze drying. Finally, the obtained mixture was calcined at 700°C under Ar/H_2 (5%) mixture gas for 5h for carbonization to obtain the 3D porous carbon (Pc). For comparison, the Si@Pc and Pc were also prepared without graphene using the same method. The scanning electron microscopy (SEM, Field Emission) was adopted to measure the morphology of the synthesized samples. The microstructure and high-resolution morphology were further analyzed by the transmission electron microscopy (TEM, JEOL JEM-2100). Raman spectra was also collected using the Thermfisher spectrometer at an excitation wavelength of 532nm. The thermogravimetry (TG) analysis was carried out from room temperature to 900°C on the instrument L75VS (Gramany) Linseis, and the BET data was collected in the ASAP 2060 system. The CR-2032 coin cells were packaged in a glove box with high purity (99.99%) argon gas and constant humidity and oxygen concentration (1ppm). The counter assemble electrode is pure Lithium foil and the separator membrane is Celgard 2300-typed organic polymer. A 1mol L^{-1} $LiPF_6$ organic solution matching the 1:1 EC and DMC solvent was used as the electrolyte. The cyclic voltammetry (CV) features were adopted on electrochemical workstation (DH7000) at a scanning rate 0.1mV s^{-1} and 0~2 scanning voltage. The electrochemical impedance spectra (EIS) in the frequency range varied from 0.1 Hz to 1MHz was also adopted through the DH7000 workstation. And the Land (Wuhan, China) battery measurement was selected to gather the discharge/charge performance curves in the required voltage range in constant temperature (300K).

3. Results and Discussion

The scanning electron microscopy (SEM) images show that the Si@Gra@Pc composites are constituted by the 3D interconnected honeycomb porous (Figure 2a-c) networks with Si nanoparticles embedded like the Jujube cake (Figure 2d and e), which boost the fast transfer of electrons and ions during the lithiation and delithiation process. Here the Si nanoparticles with a diameter of around 50 nm that below the critical size that Si particles would crack upon lithiation. The Si@Gra nanoparticles are fully encapsulated by the Pc and the Gra and Pc can prevent Si NPs to be clustered during the annealing process. This fabricated micro-nanostructure can not only improves the electronic conductivity of Si NPs, but also shorten the Li^+ ions transfer paths and maintains good electrons and ions kinetics. Mainly, three functions in the structure are followed: (a) porous skeleton can afford the mechanical stability for the designed structure; (b) the Gra and Pc can improve the electrical conductivity and mechanical stability, as well as the high permeability for the Li^+ ions; (c) Gra coating can enhance the interface contact between Si nanoparticles and Pc, and prevent Si NPs from direct exposing to the electrolyte in the time of charge/discharge process, which is beneficial to facilitate the formation of stable SEI films [30-34].

Figure 1. *Schematic technological process of CVD direct growth of few-layer Gra on the Si nanoparticles surface to form the Si@Gra core-shell nanostructure (upper); and schematic image for the freeze-drying assisted method to prepare the Si@Gra@Pc composite (down).*

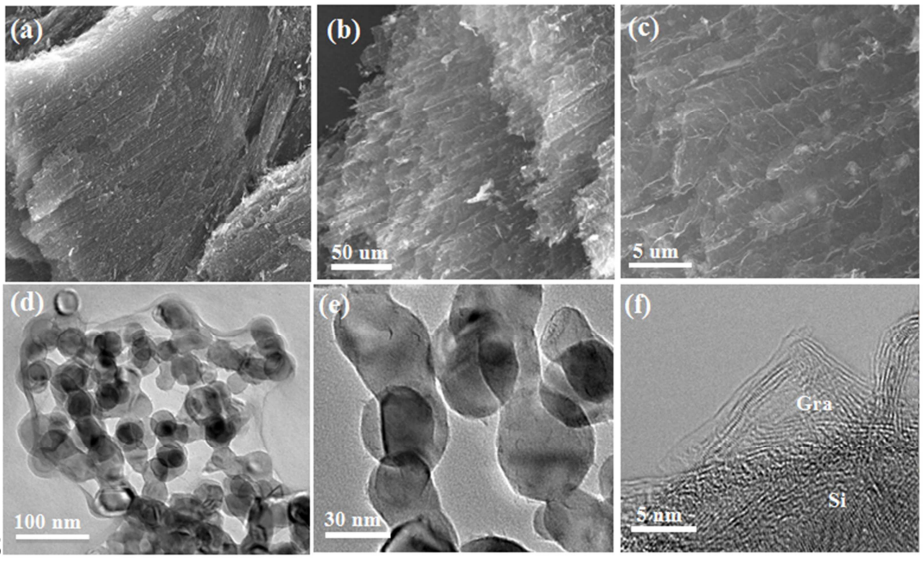

3

Figure 2. *(a-c). SEM images of honeycomb porous carbon (Pc); (d). TEM image of the walnut Si@Gra@Pc; (e). TEM image of Si@Gra; (f). HRTEM of the edge of the Si@Gra.*

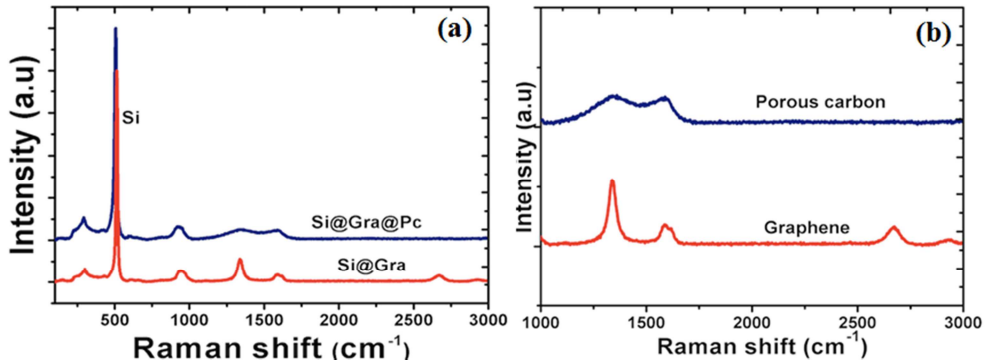

Figure 3. *(a) Raman comparison for the bare Si@Gra and Si@Gra@Pc; (b) Raman spectrum for the Pc and Gra in the wave numbers range 1000~3000 cm^{-1}.*

Figure 3 shows the Raman spectra for the synthesized samples. As indicated, in the wave number range 100~3000 cm^{-1}, the characteristic peak for the Si particle is mainly centered at ~500 cm^{-1} (Figure 3a), while the Si@Gra@Pc showed wide D (1350cm^{-1}) band and G (1580cm^{-1}) band and the Si@Gra shows obvious 2D (2700cm^{-1}) band, which is the characteristic peak for the few-layer Gra (fGra) with various layer number, in addition, the fGra synthesized on the Si nanoparticles is in the size of nanometer range, the D band intensity is increased relatively due to the enhanced Raman scattering effect in the nano-size range [34-36].

The cyclic voltammetry (CV) are accomplished to further characterize the electrochemical performance of the Si@Gra@Pcanode in a voltage range of 0.001-2V (versus Li/Li^+) at a sweep rate of 0.1 mV s^{-1}, other three anode including bare Si, Si@Gra, and Si@Pc are also included for compare (Figure 4). From the measurement results, it is shown that all the samples (excluding the pure Pc) electrodes maintained the typical features of Si as indicated in the cyclic CV curves and the lithium insertion mainly occurs at the work potential below 0.3V. More important, the Si@Gra@Pc shows the best reversibility compared to Si@Gra and Si@Pc as shown by the narrow spacing of curves in the initial five cycles. The reduction peaks around in 0.19~0.21V corresponding to the phase change for the charging are more stable for the Si@Gra@Pc and the peak variation are distinct from the Si@Gra and Si@Pc anodes. In the anodic scans, the peaks centered at 0.35V, 0.53 V are the oxidation peaks for Li^+ ions withdraw in Si-Li alloy [22, 27-30], while the peaks at 0.16 and 0.23V in the cathodic and anodic scan, are the redox peaks due to the lithiation and delithiation of carbon in the Si-C electrode [22, 27-30], which is identified in the Pc anode (shown in Figure 4a). Figure 5a gives the TG analysis for the Si@Gra@Pc, from the measurement results, the obtained samples in the present work contained about 40% Si in the composite, and the Si@Gra contained~90% Si as described in our previous reports [28-30]. The BET analysis for the Si@Gra@Pc is also shown in Figure 5b. The surface area and porous structure for the Si@Gra@Pc are distinct from that of the Si nanoparticles, producing significant influence on the electrochemical performance, especially for the initial CE which may be the main reason for the different original CE for Si, Si@Gra and Si@Gra@Pc.

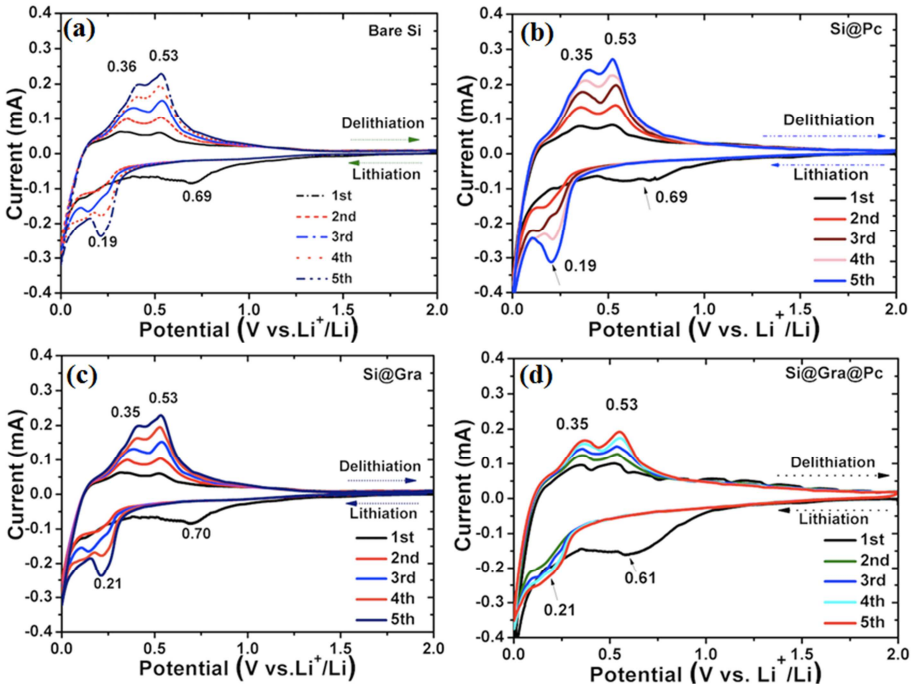

Figure 4. *Cyclic voltammetric (CV) curves of the first five cycles for a). Bare Si; b). Si@Pc; c). Si@Gra; and d). Si@Gra@Pc, at a scan rate of 0.1mV* s^{-1} *between 0 and 2.0 V.*

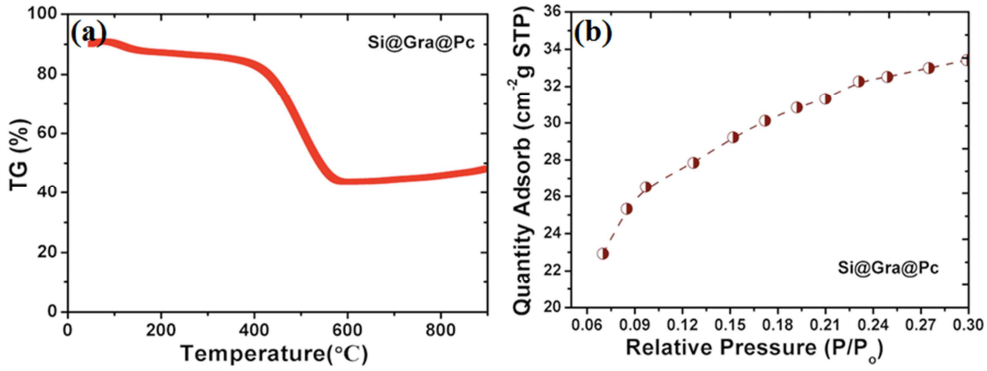

Figure 5. *(a) TG analysis of the Si@Gra@Pc; (b) BET results of the Si@Gra@Pc from room temperature to 900°C.*

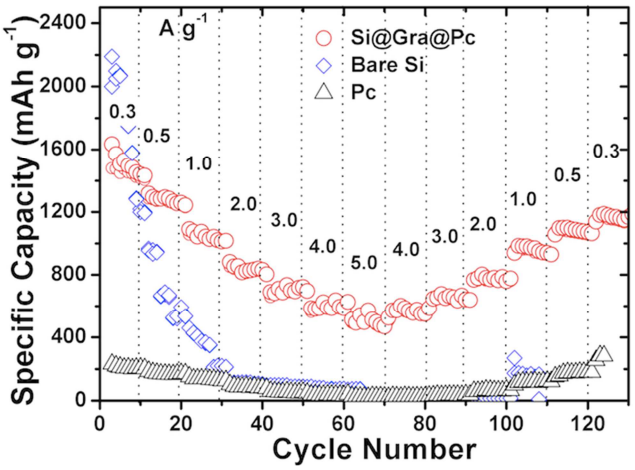

Figure 6. *Compare of the rate capability from the Si@Gra@Pc, bare Si and Pc anodes.*

The rate performance of the obtained samples were compared in Figure 6. The rate capacity was evaluated by the lithiation-delithiationprocess at varied current densities varied from 0.3 to 5.0 Ag^{-1}. Remarkably, the Si@Gra@Pc composite anode exhibits the best rate performance, compared with the bare Si and Pc anodes. The Si@Gra@Pc delivered a high average reversible discharge capacity of 1450, 1250, 1000, 800, 700, 600 and 500 mAh g^{-1} at rates of 300, 500, 1000, 2000, 3000, 4000, and 5000 mA g^{-1}, respectively. After deeper charge/discharge for 130 cycles, the specific capacity was recovered again to 1200 mAh g^{-1} when scanned at current density 300 mA g^{-1} although experiencing a series of high-rate cycles. In contrast, it was seen that the bare Si only showed a high specific capacity at low current densities for tens of cycles and subsequently the fast capacity fading with increasing the current density even to 2.0 A g^{-1}. These results further indicated that the good synergistic effects between graphene and porous carbon responsible for the remarkable enhancement of the electrochemical performance of the Si anodes. The good rate performance of Si@Gra@Pc composites was attributed to the following reasons: First, the Gra

coating layer could provide sufficient and fast electrons transportation highway; Second, the 3D-interconnected porous carbon network could support Si nanoparticles as a mechanical skeleton and maintain the structure integrated; Third, the existence of nanospace between Si nanoparticles and porous carbon could shorten the pathways for Li^+ transfer and enhance the Li^+ diffusion to the Si particles, as well as release the deformation stress generated in thelithiation and delithiation process.

The electrochemical impedance spectroscopy (EIS) was performed in order to further explore the ions diffusion and charge transfer between the bare Si and Si@Gra@Pc before and after cycles. All Nyquist plots in Figure 7a exhibited the curves consisted of semicircles and straight lines in the high and low frequency regions, respectively. Compared with the bare Si, the Si@Gra@Pc anode showed a suppressive diameter of the semicircle, which indicated the increased charge transfer conductivity at the electrolyte-electrode interface due to the presence of high-conductance Gra layer. Moreover in the low frequency range, the slope of the linear was increased, which indicated that the solid-state diffusion resistance of Li+ ions inside the electrode materials was reduced in the Si@Gra@Pc. Apparent, the Si@Gra@Pc showed the good diffusion kinetics that was attributed to the reinforced interface contact. Additionally, the first CE for the Si@Gra@Pc is~60%, after the initial several cycles, the CE increases to more than 99-99.8% in the subsequent cycles, and the initial CE for Si@Gra is~77%, while for Si@Pc and Pc is only~40%, and~36%, separately, which mainly ascribes to the large amounts of trapping Li^+ ions sites in the Pc.

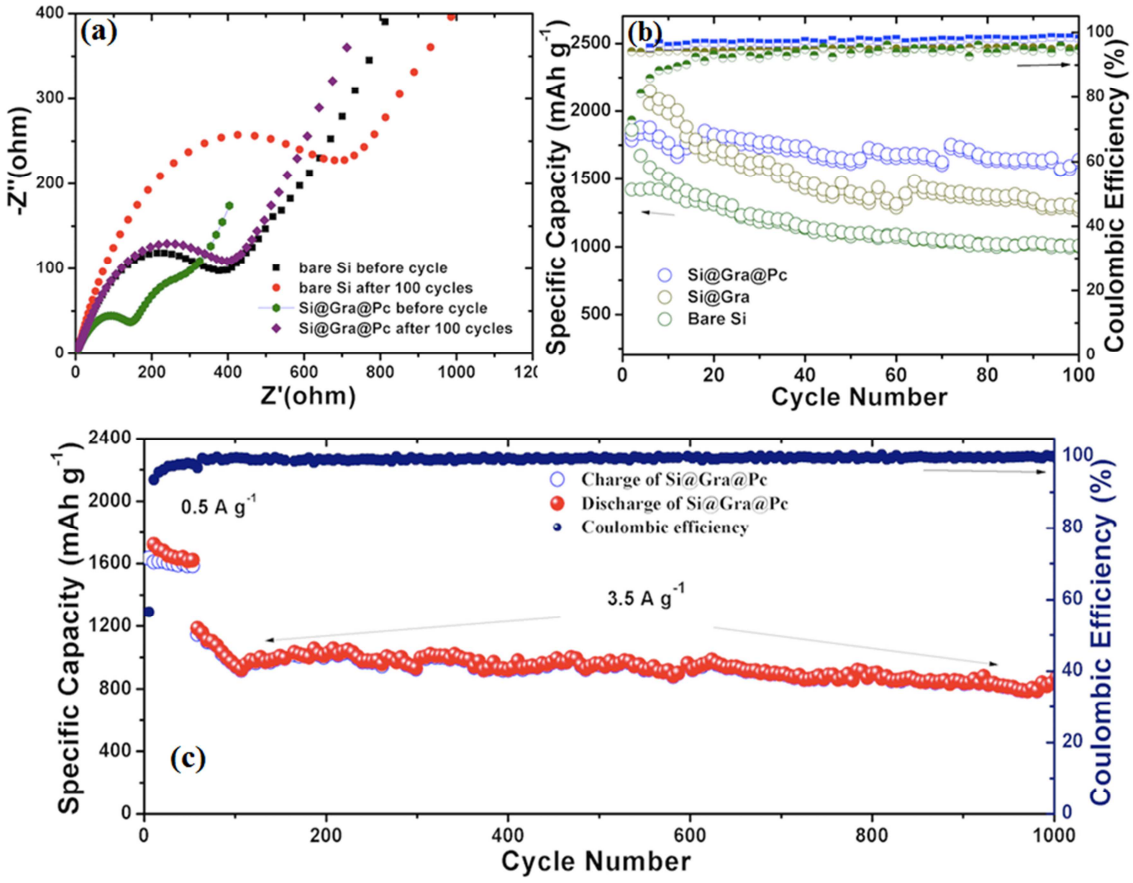

Figure 7. *(a) Nyquist plots of Si@Gra, Si@Pc and Pc electrodes before cycles, and the Si@Gra@Pc electrodes before and after 150 and 300 cycles, separately; (b) Comparison of cycling performance of the Si@Gra@Pc, Si@Gra, and bare Si at different current densities, Coulombic efficiency of the different composite anodes is exhibited as well; (c) The cycling performance of the Si@Gra@Pc at current density of 3.5 A* g^{-1}.

The CE and cycling performance at 0.2C and 2.0C (C=3500 mAh g^{-1}) are shown in Figure 7b. It should be noted that all specific capacity present in this work are calculated based on the mass of Si in the Si-C composites. The capacity contribution from Gra and Pc is about 50~100 mAh g^{-1} and 120~160 mAh g^{-1}, separately. Different samples are compared (Figure 7b) and it is evident that the Si@Gra@Pc shows the best cycling stability even at 2C current density, while the bare Si anode undergo rapid capacity decay during the initial cycles and then keeps continuously decreasing in the subsequent cycles even at current density of 0.2C. The Si@Gra@Pc anode (Figure 7c) display stable cycle ability even experiencing 1000 cycles at current density 3.5A g^{-1}. Compared with Figure 7b, the Si@Gra@Pc could keep stable cycling at varied current density not only at 7.0Ag^{-1} but also at 3.5Ag^{-1}. Without the addition of other special assistances, such as electrolyte additives, the long cycle life and high capacity of Si@Gra@Pc are attributed to the unique designed structure and the nature specialties of the anode materials. The Si@Gra@Pcelectrode architectures capitalize the merits of superior high capacity silicon and

unique physical properties of Gra and Pc network, synergistically, which serve as transport highway for charges and stable mechanical support for the active particles that providing good rate capability and cycling stability for the fabricated anode. In particular, the few-layer CVD growth Gra act as an electrolyte protective layer and the 3D-interconnected Pc matrix with hollow interior spaces function as effective charges highway and support backbone for active particles to effectively relieve the volume expansion strain during the lithium insertion/extraction process and maintain the entire electrical connection integrity.

4. Conclusion

In summary a novel Si-C tectonism anode is designed and synthesized via predigest method by convenient freeze-drying-assisted strategy associated with CVD method. This architecture, combining the properties of a porous structure and an electron high-speed conductive elastic skeleton, can provide bi-continuous ion-electron pathways. The results demonstrate that the electrode made of the as-designed Si@Gra@Pc has good rate capability and long cycle stability. The proposal is not only operation-convenient but also cost-effective, and therefore it is highly expected for scaled-up production. In addition, this anode composite can withstand the damage on the rate performance of LIBs cycling at 5.0 Ag^{-1} after 130 cycling and stable cycling even after 1000 cycles at 3.5 A g^{-1} current density. Such a highly interconnected structure could provide effective strategy for the large-scale production Si-based anode materials for LIBs applications. The double effect from Gra and Pc, with which they can sustain large strain without pulverization, can afford unexceptionable electrical conduction and shorten lithium transfer distances.

Acknowledgements

We sincerely express our appreciation to the support from the National Natural Science Foundation of China (Grant No. 11604245, 11874282, 11981240429) Six Top Talent in Jiangsu Province (Grant No. XNY-074), and the Scientific Research Start Funding From Jiangsu University of Science and Technology (Grant No. 1052931707).

References

[1] M. Zeringer, J. Price, B. Fais, P. H. Li, and E. Sharp, “Designing low-carbon power systems for Great Britain in 2050 that are robust to the spatiotemporal and inter-annual variability of weather,” Nature Energy, vol. 3, pp. 395-403, 2018.

[2] Y. F. Zhang, P. X. Wang, T. Zheng, D. M. Li, G. D. Li, and Y. Z. Yue, “Enhancing Li-ion battery anode performance via disorder/order engineering,” Nano Energy, vol. 49, pp. 596-602, 2018.

[3] G. L. Hou, B. L. Cheng, Y. J. Yang, Y. Du, Y. H. Zhang, B. Q. Li, J. P. He, Y. Z. Zhou, D. Yi, N. N. Zhao, Y. Bando, D. Golberg, J. N. Yao, X. Wang, and F. L. Yuan, “Multiscale Buffering Engineering in Silicon-Carbon Anode for Ultrastable Li-Ion Storage,” ACS Nano, vol 13, pp. 10179-10190.

[4] A. S. Arico, P. Bruce, B. Scrosati, J. M. Tarascon, and W. V. Schalkwijk, “Nanostructured materials for advanced energy conversion and storage devices,” Nature Materials, vol. 4, pp. 366-377, 2005.

[5] J. Cabana, L. Monconduit, D. Larcher, andM. R. Palacin, “Beyond intercalation-based Li-ion batteries: The state of the art and challenges of electrode materials reacting through conversion reactions,” Advanced Materials, vol. 22, pp. 170-192, 2010.

[6] Y. L. An, Y. Tian, L. J. Ci, S. L. Xiong, J. K. Feng, and Y. T. Qian, “Micron-Sized Nanoporous Antimony with Tunable Porosity for High Performance Potassium-Ion Batteries,” vol. 12, pp. 12932-12940, 2018.

[7] A. Ladam, N. Bibent, C. Cénac-Morthé, L. Aldon, J. Olivier-Fourcade, J. -C. Jumas, P. -E. Lippens, “One-pot ball-milling synthesis of a Ni-Ti-Si based composite as anode material for Li-ion batteries,” vol. 245, pp. 497-504, 2019.

[8] Seung-Su Lee, Ki-Hun Nam, Heechul Jung, Cheol-Min Park, “Si-based composite interconnected by multiple matrices for high- performance Li-ion battery anodes,” Chemical Engineering Journal, vol. 381, 122619, 2020.

[9] X. Q. Liang, J. J. Wang, S. Y. Zhang, L. Y. Wang, W. F. Wang, L. Y. Li, H. F. Wang, D. Huang W. Z. Zhou, J. Guo, “Fabrication of uniform Si-incorporated SnO_2 nanoparticles on graphene sheets as advanced anode for Li-ion batteries,” Applied Surface Science, vol. 476, 28-35, 2019.

[10] J. R. Szczech, and S. Jin, “Nanostructured silicon for high capacity lithium battery anodes,” Energy &Environmental Science, vol. 4, pp. 56-72, 2011.

[11] C. K. Chan, H. L. Peng, G. Liu, G. K. McIlwrath, X. F. Zhang, R. A. Huggins, and Y. Cui, “High performance lithium battery anodes using silicon nanowires,” Nature Nanotechnology, vol. 3, pp. 31-35, 2008.

[12] H. Wu, and Y. Cui, “Designing nanostructured Si anodes for high energy lithium ion batteries,” Nano Today, vol. 7, pp. 414-429, 2012.

[13] Y. Tian, Y. L. An, and J. K. Feng, “Flexible and Free-Standing Silicon/MXene Composite Paper for High-Performance Lithium-Ion Batteries,” ACS Appl. Mater. Interfaces, DOI：10. 1021/acsami. 8b21893. 2019.

[14] Y. L. An, H. F. Fei, G. F. Zeng, L. J. Ci, S. L. Xiong, J. K. Feng, and Y. T. Qian, “Green, Scalable, and Controllable Fabrication of Nanoporous Silicon from Commercial Alloy Precursors for High-Energy Lithium-Ion Batteries,” ACS Nano, vol. 12, pp. 4993-5002, 2018.

[15] S. L. Jing, H. Jiang, Y. J. Hu, J. H. Shen, and C. Z. Li, “Face-to-face contact and open-void coinvolved Si/C nanohybrids lithium-ion battery anodes with extremely long cycle life,” Advanced Functional Materials, vol. 25, pp. 5395-5401, 2015.

[16] Y. H. Huang, Q. Bao, B. H. Chen, and J. G. Duh, “Nano-to-Microdesign of Marimo-like carbon nanotubes supported frameworks via in-spaced polymerization for high performance silicon lithium ion battery anodes,” Small, vol. 19, pp. 2314-2322, 2015.

[17] N. Liu, Z. D. Lu, J. Zhao, M. T. McDowell, H. W. Lee, W. T. Zhao, and Y. Cui, "A pomegranate-inspired nanoscale design for large-volume-change lithium battery anodes," Nature Nanotechnology, vol. 9, pp. 187-192, 2014.

[18] R. Yi, J. T. Zai, F. Dai, M. L. Gordin, and D. H. Wang, "Dual conductive network-enabled graphene/Si-C composite anode with high areal capacity for lithium-ion batteries," Nano Energy, vol. 6, pp. 211-218, 2014.

[19] C. F. Sun, H. L. Zhu, M. Okada, K. Gaskell, Y. Inoue, L. B. Hu, and Y. H. Wang, "Interfacial oxygen stabilizes composites silicon anodes," Nano Letters, vol. 15, pp. 703-708, 2015.

[20] J. B. Chang, X. K. Huang, G. H.; Zhou, S. M. Cui, P. B. Hallac, J. W. Jiang, P. T. Hurley, and J. H. Chen, "Multilayer Si nanoparticles/reduced graphene oxide hybrid as a high-performance lithium-ion battery anode," Advanced Materials, vol. 26, pp. 758-764, 2014.

[21] W. J. Lee, T. H. Hwang, J. O. Hwang, H. W. Kim, J. W. Lim, H. Y. Jeong, J. W. Shim, T. H. Han, J. Y. Kim, J. W. Choi, and S. O. Kim, "N-doped graphitic self-encapsulation for high performance silicon anodes in lithium-ion batteries," Energy &Environmental Science, vol. 7, pp. 621-626, 2014.

[22] H. Wu, G. Y. Zheng, N. Liu, T. J. Carney, Y. Yang, and Y. Cui, "Engineering empty space between Si nanoparticles for lithium-ion battery anodes,"Nano Letters, vol. 12, pp. 904-909, 2012.

[23] W. Y. Li, Y. B. Tang, W. P, Kang, Z. Y. Zhang, X. Yang, Y. Zhu, W. J. Zhang, and C. S. Lee, "Core-shell Si/C nanospheres embedded in bubble sheet-like carbon film with enhanced performance as lithium ion battery anodes," Small, vol. 11, pp. 1345-1351, 2015.

[24] B. Wang, X. L. Li, X. F. Zhang, B. Luo, Y. B. Zhang, and L. J. Zhi, "Contact-engineered and void-involved silicon/carbon nanohybrids as lithium-ion-battery anodes," Advanced Materials, vol. 25, pp. 3560-3565, 2013.

[25] X. Zhao, C. M. Hayner, M. C. Kung, and H. H. Kung, "In-Plane vacancy-enabled high-power Si-Graphene composite electrode for lithium-ion batteries," Advanced Energy Materials, vol. 1, pp. 1079-1084, 2011.

[26] X. S. Zhou, Y. X. Yin, L. J. Wan, and Y. G. Guo, "Facile synthesis of silicon nanoparticles inserted into graphene sheets as improved anode materials for lithium-ion batteries," Chemical Communications, vol. 48, pp. 2198-2200, 2012.

[27] H. Ma, F. Y. Cheng, J. Chen, J. Z. Zhao, C. S. Li, Z. L. Tao, and J. Liang, "Nest-like silicon nanospheres for high-capacity lithium storage," Advanced Materials, vol. 19, pp. 4067-4070, 2007.

[28] Y. M. Sun, N. Liu, Y. Cui, "Promises and challenges of nano materials for lithium-based rechargeable batteries," Nature Energy, vol. 71, 16071, 2016.

[29] H. Wu, G. Chan, J. W. Choi, Y. Yao, M. T. McDowell, S. W. Lee, A. Jackson, Y. Yang, L. B. Hu, and Y. Cui, "Stable cycling of double-walled silicon nanotube battery anodes through solid-electrolyte interphase control," Nature Nanotechnology, vol. 7, pp. 310-315, 2012.

[30] X. H. Liu, L. Zhong, S. Huang, S. X. Mao, T. Zhu, and J. Y. Huang, "Size-Dependent fracture of silicon nanoparticles during lithiation," ACS Nano, vol. 6, pp. 1522-1531, 2012.

[31] J. Li, and J. R. Dahn, "An in situ X-ray diffraction study of reaction of Li with crystalline Si,"Jounal of The Electrochemical Society, vol. 154, pp. A156-A161, 2007.

[32] X. L. Ding, H. F. Wang, X. X. Liu, Z. H. Gao, Y. Y. Huang, D. H. Lv, P. F. He, and Y. H. Huang, "Advanced anodes composed of graphene encapsulated nano-silicon in a carbon nanotube network," RSC Advances, vol. 7, pp. 15694-15701, 2017.

[33] X. L. Ding, X. X. Liu, Y. Y. Huang, X. F. Zhang, Q. J. Zhao, X. H. Xiang, G. L. Li, P. F. He, Z. Y. Wen, J. Li, and Y. H. Huang, "Enhanced electrochemical performance promoted by monolayer graphene and void space in silicon composite anode materials," Nano Energy, vol. 27, pp. 647-657, 2017.

[34] X. L. Ding, and Y. J. Wang, "Bilayer-graphene-coated Si nanoparticles as advanced anodes for high-rate lithium-ion batteries," Electrochimica Acta, vol. 329, 134975, 2019.

[35] H. Muramatsu, Y. A. Kim, K-S. Yang, R. C-Silva, I. Toda, T. Yamada, M. Terrones, M. Endo, T. Hayashi, and H. Saithoh, "Rice Husk-Derived Graphene with Nano-Sized Domains and Clean Edges," Small, vol. 10, pp. 2766-2770, 2014.

[36] P-C. Lin, Y-R. Chen, K -T. Hsu, T-N. Lin, K-L. Tung, J-L. Shen, and W-R. Liu, "Nano-sized graphene flakes: insights from experimental synthesis and first principles calculations," Phys. Chem. Chem. Phys., vol. 19, pp. 6338-6344, 2017.